

Strength and fracture toughness of *in situ*-toughened silicon carbide

DUK-HO CHO

Institute of Ceramic Technology, NITQ, 233-5 Gasandong, Kumcheon-ku, Seoul, Korea

YOUNG-WOOK KIM, WONJOONG KIM

Department of Materials Science and Engineering, Seoul City University, 90 Jeonnonng-Dong, Dongdaemoon-Ku, Seoul 130-743, Korea

Fine β -SiC powders either pure or with the addition of 1 wt % of α -SiC particles acting as a seeding medium, were hot-pressed at 1800 °C for 1 h using Y_2O_3 and Al_2O_3 as sintering aids and were subsequently annealed at 1900 °C for 2, 4 and 8 h. During the subsequent heat treatment, the $\beta \rightarrow \alpha$ phase transformation of SiC produced a microstructure of "*in situ* composites" as a result of the growth of elongated large α -SiC grains. The introduction of α -SiC seeds into the β -SiC accelerated the grain growth of elongated large grains during annealing which led to a coarser microstructure. The sample strength values decreased as the grain size and fracture toughness continued to increase beyond the level where clusters of grains act as fracture origins. The average strength of the *in situ*-toughened SiC materials was in the range of 468–667 MPa at room temperature and 476–592 MPa at 900 °C. Typical fracture toughness values of 8 h annealed materials were 6.0 MPa m^{1/2} for materials containing α -SiC seeds and 5.8 MPa m^{1/2} for pure β -SiC samples.

1. Introduction

Silicon carbide ceramics are of considerable interest due to their excellent oxidation, corrosion, and creep resistance properties at elevated temperatures. Silicon carbide ceramics can be fabricated by pressureless sintering with the aid of boron and carbon at temperatures in excess of 2000 °C [1]. Several investigations have shown that these SiC materials have a low fracture toughness value (2.5–4 MPa m^{1/2}) [2] and a moderate strength (350–500 MPa) [3, 4].

Recently, several reports have been published on *in situ*-toughened SiC [5–12], which is akin to Si_3N_4 . The improvement in fracture toughness was achieved through the development of elongated α -SiC grains; i.e. the higher toughness values of *in situ*-toughened materials were due to bridging by elongated grains as evidenced by R-curve behaviour, i.e. increasing crack growth resistance with crack extension [10]. The toughness properties and R-curve behaviour of *in situ*-toughened SiC have been extensively reported in the literature [6, 8, 13]. However, the strength properties of these materials have not been comprehensively studied.

In this study, various *in situ*-toughened SiC materials that possess different microstructures were prepared by hot-pressing and subsequent annealing. Their strength and fracture toughness properties are presented and correlated with their respective microstructures.

2. Experimental procedure

Commercially available β -SiC (Ultrafine, Ividen Co., Ltd, Nagoya, Japan), α -SiC (A-1, Showa Denko, Tokyo, Japan), Al_2O_3 (AKP-30, Sumitomo Chemicals, Tokyo, Japan), and Y_2O_3 (Grade Fine, H.C. Starck, Berlin, Germany) were used as the starting powders. Alpha-SiC powders were added so to act as seeds. To prepare a powder composition that did not contain any seeds, 80 wt % β -SiC was mixed with 12 wt % Al_2O_3 and 8 wt % Y_2O_3 and then the mixture was milled in a polyethylene jar containing ethanol and SiC balls for 24 h. In order to prepare a powder composition that did contain seeds, 79 wt % β -SiC was mixed with 12 wt % Al_2O_3 and 8 wt % Y_2O_3 and the mixture was milled in a polyethylene jar containing ethanol and SiC balls for 20 h. Then 1 wt % of the seeding α -SiC powder was added and the slurry was milled for 4 h. This mixed slurry was dried, sieved through a 60 mesh screen, and hot-pressed at 1800 °C for 1 h under a pressure of 20 MPa in an argon atmosphere. The hot-pressed materials were further heated at 1900 °C for 2, 4 and 8 h under an atmospheric pressure of Ar to enhance grain growth. The sample designations are given in Table 1.

The sample densities were measured using the Archimedes' method. The theoretical densities of the specimens, 3.383 g cm⁻³, were calculated according to the rule of mixtures. X-ray diffraction (XRD) was used to determine the crystalline phases present in the

TABLE I Sample designation

| Annealing time at 1900 °C (h) | Sample designation | |
|-------------------------------|--------------------------------------|-----------------------------------|
| | Material without α -SiC seeds | Material with α -SiC seeds |
| hot-pressed | A0 | B0 |
| 2 | A1 | B1 |
| 4 | A2 | B2 |
| 8 | A3 | B3 |

samples. The hot-pressed and annealed materials were cut and polished, then etched by a plasma of CF_4 containing 7.8% O_2 . The microstructures were observed by scanning electron microscopy (SEM). The hot-pressed materials were machined into $3 \times 4 \times 36$ mm bars with an 800 grit diamond wheel for flexural testing. Bend tests were performed at both room and high (900 °C) temperatures on 8 specimens at each condition using a four-point method with outer and inner spans of 30 and 10 mm, respectively and a crosshead speed of 0.5 mm per min. The fracture origin and microstructure of the fractured surfaces were observed using SEM. The fracture toughness was determined using the single-edge precracked beam (SEPB) method [14].

3. Results and discussion

3.1. Microstructure

The characteristics of both the hot-pressed and annealed SiC are summarized in Table II. The samples with a relative density of $\geq 99\%$ were produced by hot-pressing at 1800 °C with a hold time of 1 h. However, prolonged annealing at 1900 °C resulted in a decrease in the relative density, which is probably due to the formation of volatile components such as Al_2O_3 , SiO , and CO [15, 16].

The microstructures of the hot-pressed and annealed materials are shown in Fig. 1(a–h). Silicon carbide grains are etched away by the CF_4 plasma, thus these microstructures are delineated by the grain-boundary glassy phase. The microstructures of the hot-pressed materials (A0 and B0) consisted of fine, equiaxed SiC grains and a small number of relatively large grains. When the annealing time was increased,

the microstructure changed from equiaxed to elongated grains, the fraction of the $\beta \rightarrow \alpha$ phase transformation increased, and the size and aspect ratio of the grains increased. The true shape of elongated grains is considered as being plate-shaped (Fig. 2(a–h)). This tendency suggests that the grain growth predominantly proceeded along the direction of the plate, i.e. along basal planes of the grains, and was related to the $\beta \rightarrow \alpha$ phase transformation of SiC during annealing. As shown in Fig. 1(a–h), elongated grains appeared after 4 h of annealing in the materials without α -SiC seeds – i.e. A2 and A3 – and 2 h annealing of the materials with α -SiC seeds – i.e. B1 to B3. Grain growth in the A materials was therefore slower than in the B materials. The microstructure of the A3 sample solely consisted of elongated grains that were almost of the same shape as those of B3 but with a different grain size. A kind of “*in situ* composite” has been developed in both the A3 and B3 samples as a result of the bimodal distribution of grains, which is similar to the recently reported microstructure for a SiC sample that displayed high toughness values [5, 7].

As is shown in Fig. 1(a–h), the materials containing the α -SiC seeds have a relatively coarse microstructure as compared to those of the seedless materials. In the seedless materials, only large β -SiC particles acted as nuclei for the growth of large grains during the hot-pressing, since the growth of SiC grains was controlled by Ostwald ripening [17], i.e. the solution of β -SiC grains that are smaller than the critical size, mass transport by diffusion through the liquid, and reprecipitation on β -SiC grains that are larger than the critical size. In contrast, the grain growth of SiC grains in materials containing α -SiC seeds may have resulted from the overgrowth of β -SiC on α -SiC cores during the hot-pressing at the low temperature of 1800 °C, where β -SiC is possibly stable or the $\beta \rightarrow \alpha$ phase transformation may be very slow. Another possibility is that strain at the α/β interface may have caused the overgrowth of β -SiC on the α -SiC cores, thereby accelerating the growth of elongated grains during annealing [18, 19]. Hence, the differences in grain sizes observed between materials that contained seeds and the pure materials might be due to differences in the grain growth behaviour.

Phase analysis of the hot-pressed samples (A0 and B0) by XRD showed that the major phase in each

TABLE II Properties of both the hot-pressed and annealed SiC

| Material | Relative density (%) | Crystalline phase | | Flexural strength | | Fracture toughness ($\text{MPa m}^{1/2}$) |
|----------|----------------------|-------------------|--|------------------------|----------|---|
| | | Major | Trace | Room temperature (MPa) | 900 °C | |
| A0 | 99.3 | β -SiC | YAG ^a , α - Al_2O_3 | 625 ± 55 | 538 ± 47 | 3.1 ± 0.1 |
| A1 | 98.7 | β -SiC | α -SiC, YAG, α - Al_2O_3 | 585 ± 35 | 510 ± 31 | 3.7 ± 0.2 |
| A2 | 97.2 | α -SiC | β -SiC, YAG, α - Al_2O_3 | 555 ± 33 | 577 ± 38 | 4.5 ± 0.2 |
| A3 | 95.9 | α -SiC | β -SiC, YAG | 550 ± 46 | 589 ± 35 | 5.8 ± 0.3 |
| B0 | 99.1 | β -SiC | α -SiC, YAG, α - Al_2O_3 | 667 ± 37 | 592 ± 24 | 3.2 ± 0.2 |
| B1 | 97.9 | β -SiC | α -SiC, YAG, α - Al_2O_3 | 569 ± 42 | 523 ± 34 | 3.9 ± 0.2 |
| B2 | 96.6 | α -SiC | β -SiC, YAG, α - Al_2O_3 | 538 ± 39 | 536 ± 20 | 5.2 ± 0.2 |
| B3 | 95.3 | α -SiC | β -SiC, YAG | 468 ± 29 | 476 ± 19 | 6.0 ± 0.1 |

^a $\text{Al}_3\text{Y}_3\text{O}_{12}$ (yttrium aluminium garnet)

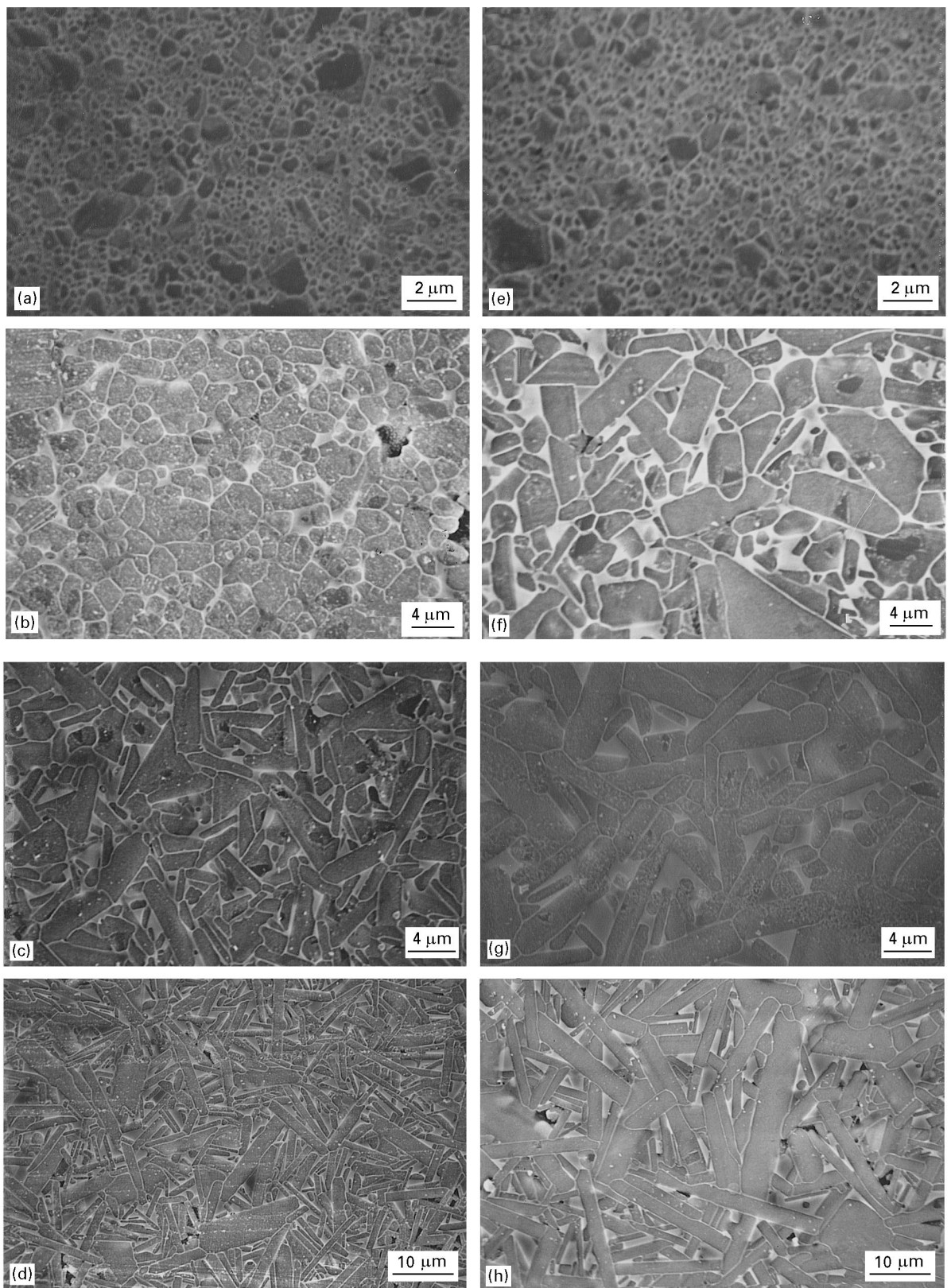


Figure 1 Microstructures of hot-pressed and annealed materials: (a) A0, (b) A1, (c) A2, (d) A3, (e) B0, (f) B1, (g) B2 and (h) B3 (refer to Table I).

sample was β -SiC (Table II). These results reveal that the growth of large grains in the A0 sample was mainly a result of overgrowth of β -SiC on the larger grains. The sample containing α -SiC seeds (B0) contained trace amounts of 6H (α -SiC) that originated from the α -SiC seeds. The 8 h annealed sample that did not contain α -SiC seeds (A3) had 4H (α -SiC) as

its major phase with trace amounts of 3C (β -SiC) being observed. In contrast, the 8 h annealed sample that did contain α -SiC seeds had 6H as its major phase with trace amounts of 3C. The XRD results indicated that the growth of elongated grains is directly related to the $\beta \rightarrow \alpha$ phase transformation of SiC.

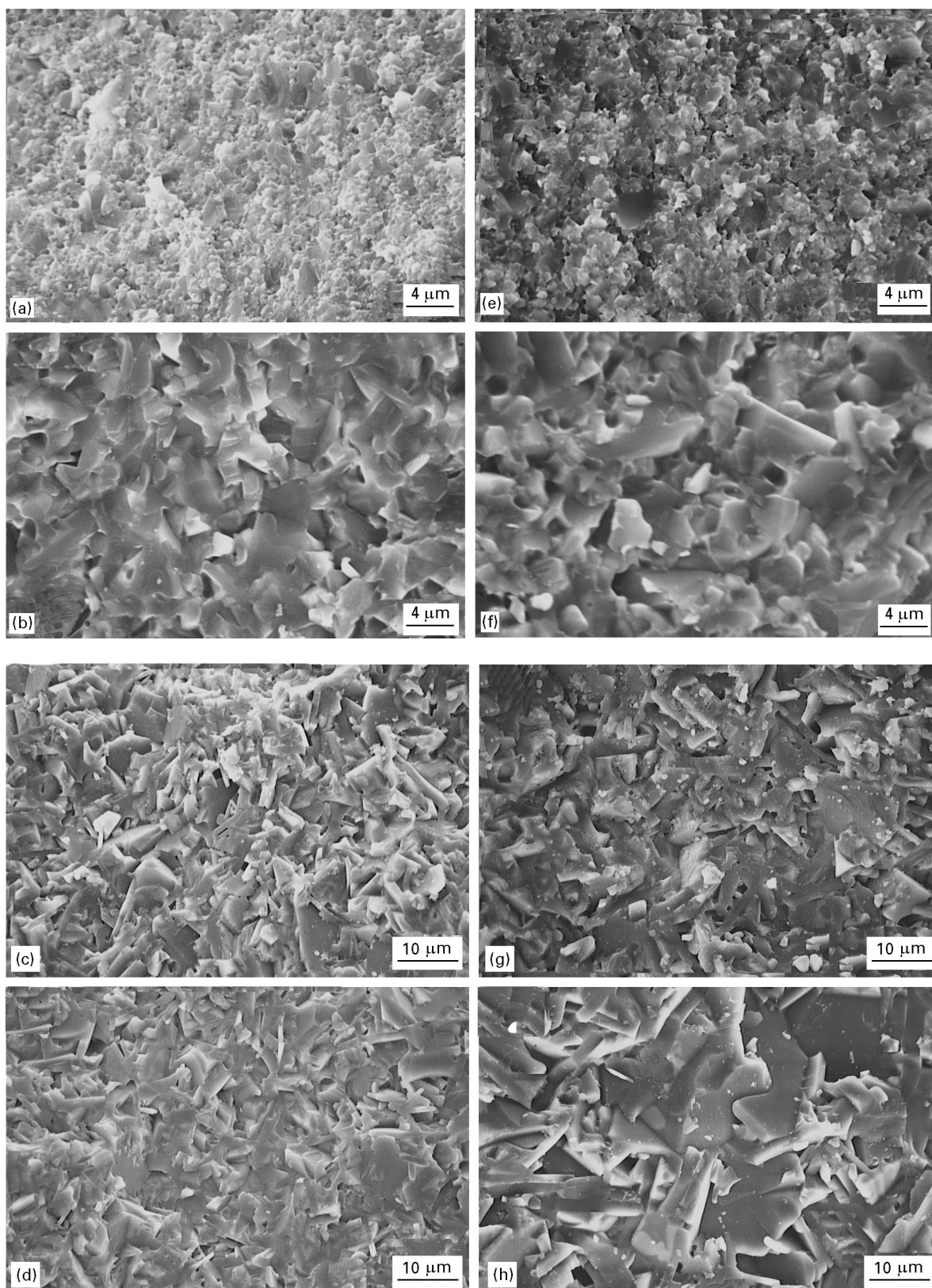


Figure 2 SEM micrographs of the fracture surfaces of hot-pressed and annealed materials: (a) A0, (b) A1, (c) A2, (d) A3, (e) B0, (f) B1, (g) B2 and (h) B3 (refer to Table I).

3.2. Mechanical properties

Fig. 2(a–h) shows SEM micrographs of the fracture surfaces of SiC ceramics with various microstructures. It has been recognized that the fracture mode in boron- and carbon-doped SiC is transgranular due to a strong grain boundary [2]. In contrast, in the case of

SiC with added Al_2O_3 and Y_2O_3 , the fracture mode is a mixture of transgranular and intergranular, as is shown in Fig. 2(e–h) which is a result of a weak interface created by the difference between the coefficients of thermal expansion of the liquid and the matrix on cooling after sintering [5]. There is a substantial

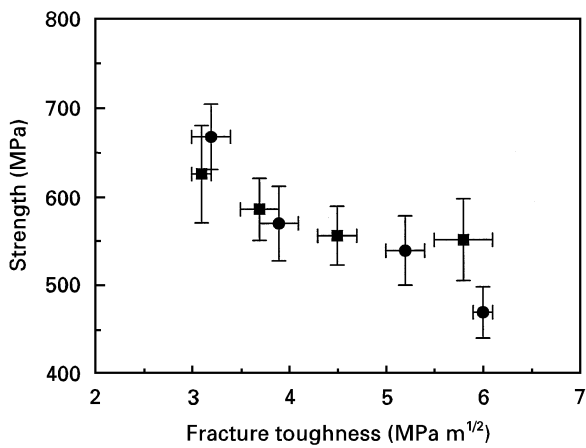


Figure 3 Relation between strength and fracture toughness of hot-pressed and annealed SiC. Key: (■) SiC without α SiC seeds and (●) SiC with α SiC seeds.

tendency for relatively larger grains to fracture transgranularly.

Fig. 3 shows the fracture toughness–strength relations for SiC ceramics that have been hot-pressed and subsequently annealed for different times, i.e. they have different microstructures. The hot-pressed materials (A0 and B0), that are composed of relatively fine, equiaxed grains, have fracture toughness values of 3–3.5 MPa m^{1/2} and a flexural strength of 600–700 MPa. In contrast, the 8 h annealed materials, that are composed of relatively large, elongated grains, have fracture toughness value of 5.5–6 MPa m^{1/2} and a flexural strength of 450–550 MPa. The effect of annealing becomes apparent after 4 h, which indicated, referring to the phase analysis in Table II, the marked growth of elongated α -SiC which produced the improved fracture toughness values and the decreased strength. The improvement in the fracture toughness is directly related to the microstructure and is produced by crack bridging by elongated SiC grains (Fig. 4(a and b)). Thus, coarser microstructures are beneficial for producing improvements in the toughness. On the other hand, a finer microstructure containing a minimal amount of small defects is required to produce improvements in the strength. Typical fracture origins were clusters of large grains and pores near the surface as is shown in Fig. 5(a and b). However, more frequently, clusters of large grains, were observed to act as fracture origin in the 8 h annealed materials. These results indicate that there is a trade-off in improving both the fracture toughness and strength. Thus it appears difficult to simultaneously achieve both a high fracture toughness and strength.

No degradation in the high-temperature flexural strength values (Table II), were observed upto 900 °C in the 4 and 8 h annealed materials (A2, A3, B2, B3), that contained elongated grains. However significant degradation was observed in the hot-pressed and 2 h annealed materials (A0, A1, B0, B1), that contained large amounts of equiaxed grains. The degradation may be due to the presence of glassy grain-boundary phases in the Al₂O₃ and Y₂O₃-doped materials. These

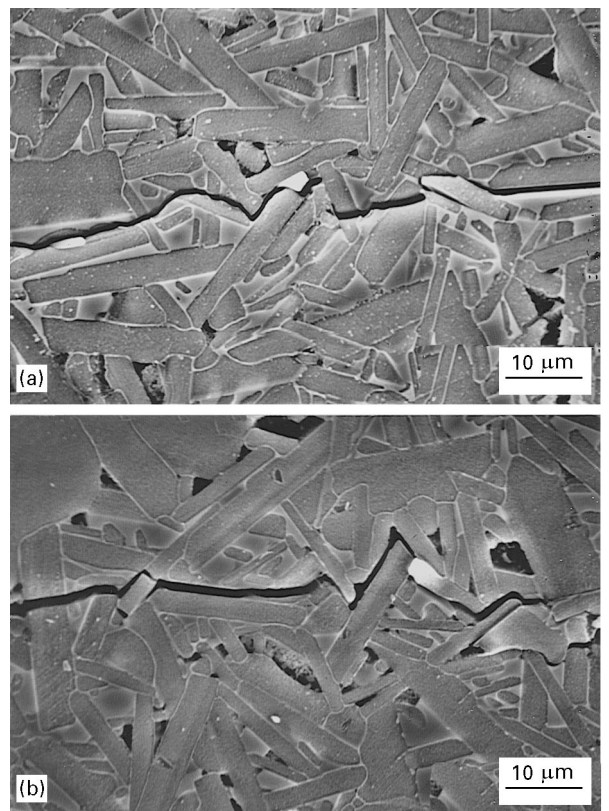


Figure 4 SEM view of crack bridging by elongated large grains in (a) A3 to (b) B3 (refer to Table I).

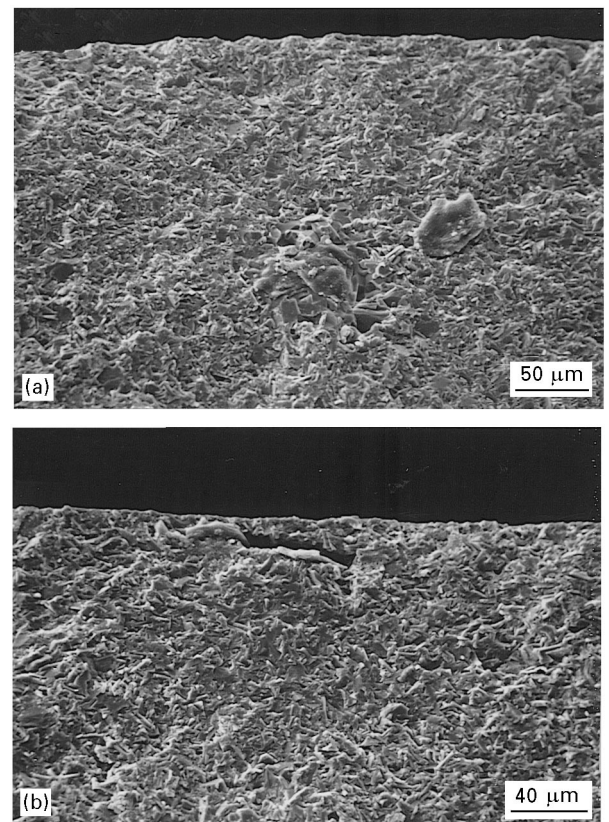


Figure 5 SEM fractography of *in situ*-toughened SiC (A3) showing typical fracture origin: (a) clusters of elongated large grains and (b) a large void.

results also suggest that the presence of plate-shaped, elongated grains prevents degradation in the strength at high-temperatures due to the interlocking of those grains.

4. Conclusions

The introduction of α -SiC seeds into β -SiC doped with Y_2O_3 and Al_2O_3 as sintering aids accelerated the grain growth of plate-shaped, elongated large grains during annealing and led to a coarser microstructure.

The room temperature-strengths of the *in situ*-toughened SiC decreased as the grain size and fracture toughness values continued to increase beyond the level where clusters of grains act as fracture origins. It has been shown that the improvement in the fracture toughness mainly arises from crack bridging by elongated SiC grains. The presence of plate-shaped, elongated grains prevented degradation of the strength at high-temperatures (900 °C) due to the interlocking of those grains.

The average strength of *in situ*-toughened SiC materials was in the range 468–667 MPa at room temperature and 476–592 MPa at 900 °C. Typical fracture toughness values for the 8 h annealed materials were 6.0 MPa m^{1/2} for materials with α -SiC seeds and 5.8 MPa m^{1/2} for materials without α -SiC seeds.

Acknowledgement

We gratefully acknowledge helpful discussions with Dr M. Mitomo (National Institute for Research in Inorganic Materials, Tsukuba, Japan).

References

1. S. PROCHAZKA, in "Special Ceramics 6," edited by P. Popper (British Ceramic Research Association, Manchester, 1975) p. 171.
2. Y. W. KIM and J. G. LEE, *J. Mater. Sci.* **27** (1992) 4746.
3. J. B. HURST and S. DUTTA, *J. Amer. Ceram. Soc.* **70** (1987) C-303.
4. S. DUTTA, *ibid* **71** (1988) C-474.
5. N. P. PADTURE, *ibid* **77** (1994) 519.
6. N. P. PADTURE and B. R. LAWN, *ibid* **77** (1994) 2518.
7. V. D. KRSTIC, *MRS Bull.* **20** (1995) 46.
8. M. A. MULLA and V. D. KRSTIC, *Acta Metall. Mater.* **42** (1994) 303.
9. S. K. LEE and C. H. KIM, *J. Amer. Ceram. Soc.* **77** (1994) 1655.
10. Y. W. KIM, M. MITOMO and H. HIROTSURU, *ibid* **78** (1995) 3145.
11. W. J. KIM and Y. W. KIM, *J. Kor. Ceram. Soc.* **32** (1995) 1162.
12. Y. W. KIM, K. S. CHO and J. G. LEE, *Kor. J. Ceram.* **2** (1996) 39.
13. S. K. LEE, D. K. KIM and C. H. KIM, *J. Amer. Ceram. Soc.* **78** (1995) 65.
14. T. NOSE and T. FUJII, *ibid* **71** (1988) 328.
15. Y. W. KIM, H. TANAKA, M. MITOMO and S. OTANI, *J. Ceram. Soc. Jpn.* **103** (1995) 257.
16. Y. W. KIM and J. G. LEE, *J. Amer. Ceram. Soc.* **72** (1989) 1333.
17. L. S. SIGL and H. J. KLEEBE, *ibid* **76** (1993) 773.
18. L. U. OGBUJI, T. E. MITCHELL, A. H. HEUER and S. SHINOZAKI, *ibid* **64** (1981) 100.
19. L. U. OGBUJI, T. E. MITCHELL and A. H. HEUER, *ibid* **64** (1981) 91.

Received 9 August 1996

and accepted 21 March 1997